CROATICA CHEMICA ACTA
CCACAA **77** (1–2) 371–376 (2004)

ISSN-0011-1643
CCA-2938
Original Scientific Paper

Ab initio Hartree-Fock Investigation of 2-Methylindole-3-acetic Acid*

Michael Ramek[a,] and Sanja Tomić[b]**

[a]*Institut für Physikalische und Theoretische Chemie, Technische Universität, A-8010 Graz, Austria*

[b]*Institut Ruđer Bošković, P. O. BOX 180, HR-10002 Zagreb, Croatia*

RECEIVED MAY 16, 2003; REVISED OCTOBER 28, 2003; ACCEPTED OCTOBER 28, 2003

The potential energy surface (PES) of 2-methylindole-3-acetic acid (2-Me-IAA) has been investigated *via* RHF/6-31G* and RHF/6-31++G** calculations. With both basis sets, only three symmetry unique local minima with *syn* orientation of the COOH group are contained in the PES. A network of reaction paths connects these energy minima. One symmetry unique energy minimum has an extremely low barrier to the adjacent global minimum. Comparison with unsubstituted IAA and its alkylated as well as halogenated derivatives substituted at positions 4, 5, 6, and 7 shows that the PES of 2-Me-IAA is quite different. This is in accord with its significantly lower auxin activity and weaker binding to auxin binding protein 1 (ABP1).

Key words
auxin
substituent effect
shape of potential energy surface
indole-3-acetic acid

INTRODUCTION

Auxin plant hormones govern many biological processes in higher plants such as cell divisions and enlargement, differentiation, morphogenesis, and the syntheses of specific proteins.[1,2] Among this class of plant hormones we are specifically interested in compounds, whose parent compound is indole-3-acetic acid (IAA), a wide spread natural auxin. IAA and some of its halogenated derivatives are naturally occuring auxins. In addition, a large number of synthetic IAA conjugates and derivatives of different degrees of activity have been tested experimentally on various plant cultures.[3–19] According to investigations performed in the second half of the last century, transport of auxins is polar; auxin molecules move along the electrochemical gradient and they enter the cell in neutral form. Recently, auxin transport proteins, so-called influx and efflux carriers, were identified. The asymmetric distribution of the carriers in the cell membrane seems to regulate auxin transport.[20]

During the recent years, we have performed *ab initio* RHF structure investigations of IAA and several chlorinated, methylated, and ethylated derivatives.[21–26] The initial idea of these studies was to find possible correlations between biological activity and characteristic data of the various potential energy surfaces. In general, such correlation is not very obvious: chlorination or ethylation at positions 5, 6, or 7 (*cf.* Figure 1) has only marginal effect upon reaction paths and potential barriers,[23,24] whereas the biological activity is spread in a wide range for these compounds.[10–19] In contrast, substitution at position 4 turned out to significantly influence the shape of the potential energy surface (PES).[27] Recently the crystal structure of the ABP1, the major candidate for auxin receptor was determined.[34] The protein is dimer in both crystal and solution; each monomer consists of 160 amino acid residues. The binding pocket of ABP1 is predominantly hydrophobic with a metal ion deep inside the pocket coordinated by three histidines and a glutamate.

---

* Dedicated to Professor Nenad Trinajstić on the occasion of his 65th birthday.

** Author to whom correspondence should be addressed. (E-mail: ramek@ptc.tu-graz.ac.at)

TABLE I. Torsion angles (degree), relative energies (kJ mol^{-1}), and imaginary frequencies (cm^{-1}) for all symmetry unique stationary points of the 2-Me-IAA 6-31G* PES with *syn* orientation of the COOH group. Zero relative energy corresponds to an absolute energy of –627.1625767 Hartree. The superscript »m« is used to denote mirror images. T1, T2, and T3 are the torsion angles C2–C3–C8–C9, C3–C8–C9=O, and H–C10–C2–N1, respectively.

	T1	T2	T3	E_{rel}	ν_1	ν_2	ν_3
A	86.539	–95.343	172.439	0.000			
B	106.239	103.404	179.236	0.142			
C	76.234	–31.241	–171.738	3.003			
A↔B	101.546	–177.556	–178.857	8.431	41.58*i*		
B↔C	107.346	42.148	179.979	6.141	35.53*i*		
A↔C	80.313	–45.355	–176.491	3.073	21.27*i*		
A↔B^m	173.011	–89.867	178.189	24.016	68.55*i*		
A^m↔C	4.854	84.814	–8.985	17.322	45.79*i*		
	0.000	0.000	0.000	23.065	66.10*i*	14.78*i*	
	0.000	0.000	180.000	24.967	66.24*i*	28.71*i*	
	0.000	180.000	0.000	39.170	75.81*i*	68.23*i*	
	0.000	180.000	180.000	43.865	105.36*i*	80.82*i*	52.61*i*
	180.000	0.000	180.000	31.449	93.70*i*	33.28*i*	
	180.000	180.000	0.000	47.910	120.58*i*	69.26*i*	
	180.000	180.000	180.000	48.063	118.28*i*	71.62*i*	21.99*i*

Rescher *et al*. showed that the ability of auxin related molecules to bind to ABP1 is correlated with their biological activity. This finding, together with significant differences in binding of 2-Me-IAA in comparison with IAA and 4-alky-IAA prompted our investigations of this compound. The present contribution describes the investigation of the PES of 2-methylindole-3-acetic acid (2-Me-IAA).

According to the experimental data[29,30] available, 2-Me-IAA is at the borderline between strong and weak auxins. Its half-optimal concentration is about ten times larger than for unsubstituted IAA and its derivatives alkylated in positions 4, 5, 6 and 7. Its binding to ABP1 is almost two orders of magnitude less effective than IAA and 4-Me-IAA.[29] Besides for 2-Me-IAA, biological measurements have been accomplished for 2-Ethyl-IAA and 2-Propyl-IAA as well.[30] Although their half optimal concentration is similar to that of 2-Me-IAA, their optimal response is only half of the 2-Me-IAA response.

COMPUTATIONAL DETAILS AND NOTATION

The position of the carboxyl group relative to the indole ring depends on two torsion angles called T1 and T2 in the following. Using the atom numbering shown in Figure 1, T1 is the torsion angle C2–C3–C8–C9 and T2 is the torsion angle C3–C8–C9=O. In addition to these, T3 will be used to denote the torsion H–C10–C2–N1. Calculations were performed with the program GAMESS[31] on a variety of machines. The standard basis sets 6-31G* and 6-311++G** with six d-functions were employed as coded in GAMESS. The standard RHF procedure[32] was used throughout.

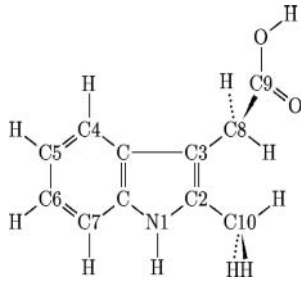

Figure 1. Atom numbering used for 2-Me-IAA.

Only conformers with the COOH group in *syn* orientation were considered, since the corresponding *anti* conformers turned out to be around 30 kJ mol^{-1} less stable in previous studies. The *syn* section of the 2-Me-IAA PES was first mapped in detail: restricted RHF/6-31G* optimizations were carried out on a regular grid with T1 = 0, 20, 40, …, 180° and T2 = –160, –140, –120, …, 180°. After completion of this grid, stationary points were refined in unrestricted RHF/6-31G* and RHF/6-311++G** geometry optimizations.

All structures were fully optimized to a remaining root mean square (rms) gradient less than 0.33 x 10^{-4} Hartree/Bohr. The nature of all stationary points was verified *via* computation of the eigenvalues of the Hessian matrix: local minima had only positive eigenvalues, transition states had exactly one negative eigenvalue, and second order transition states had exactly two negative eigenvalues.

RESULTS

Initially, the investigation was carried out with the 6-31G* basis set, since this basis set has been proven to be adequate in the case of IAA.[21]

Three symmetry unique (*i.e*., T1 ≥ 0°) local minima with *syn* orientation of the COOH group were located in the PES, which are labelled **A**, **B**, and **C** in the following, according to increasing energy. Furthermore, there are

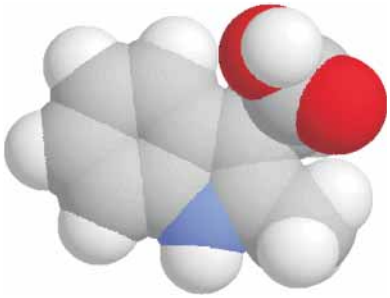

Figure 2. Fused sphere model of energy minimum A.

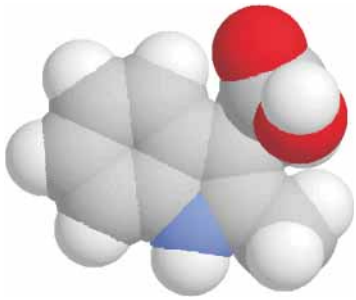

Figure 3. Fused sphere model of energy minimum B.

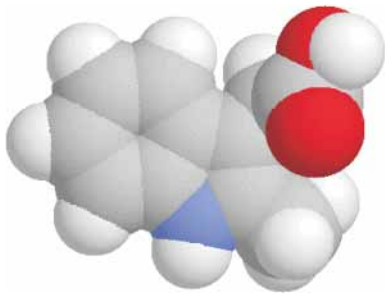

Figure 4. Fused sphere model of energy minimum C.

five symmetry unique transition states, and four symmetry unique second order transition states with *syn* orientation of the COOH group. The values of T1, T2, T3, the energies, and the imaginary frequencies of these stationary points are collected in Table I. The geometry of the symmetry unique energy minima is shown in Figures 2–4.

Two low energy paths with T1 ≈ ± 100° connect the energy minima **A**–**C**–**B**–**A** and their mirror images $\mathbf{A^m}$–$\mathbf{C^m}$–$\mathbf{B^m}$–$\mathbf{A^m}$, respectively. In addition, there are two paths **B**–$\mathbf{A^m}$–**C** and $\mathbf{C^m}$–**A**–$\mathbf{B^m}$, in which T1 and T2 perform a combined motion (with increasing values of T1). Figure 5 shows these reaction paths in T1/T2-space. »Reaction path following« was used for the **B**–$\mathbf{A^m}$ section to verify that the transition state indeed connects to $\mathbf{A^m}$ and not to $\mathbf{C^m}$.

A major aspect of the 6-31G* results is the extremely low barrier of 5.9 cm^{-1} for the **C**→**A** reaction. The vibration mode of **C** that corresponds to this reaction path has an unscaled, harmonic frequency of 25.5 cm^{-1}. This means that the vibrational ground state of **C** has an energy that is above the potential barrier in the **C**→**A** reaction.

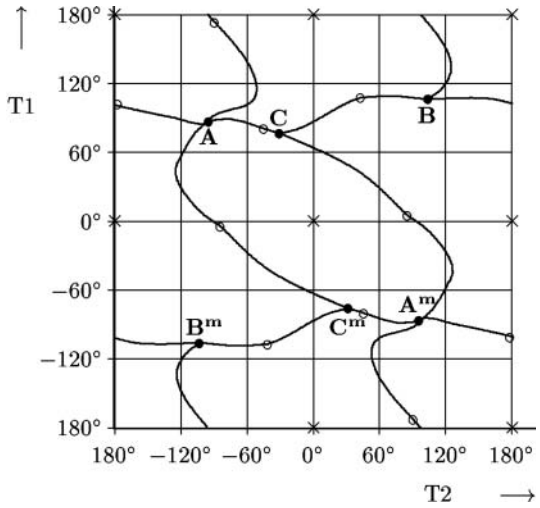

Figure 5. Stationary points and reaction paths of 2-methylindole-3-acetic acid with *syn* orientation of the COOH group. Local minima (•), saddle points (o), and second order saddle points (×). (T1 and T2 are the torsion angles C2–C3–C8–C9 and C3–C8–C9=O, respectively).

In view of this small barrier, all energy minima and transition states were reoptimized with the 6-311++G** basis set. The characteristic data with this large basis set are collected in Table II. The inclusion of additional basis functions yields slight changes of the results: most torsion angles change in the range of 1° to 2°, with a few exceptions: T1 (4°) and T3 (7.3°) in **A**, T1 (3.3°) in **B**↔**C**, T1 (6.4°) and T3 (3.5°) in **A**↔**B**, and T3 (5.5°) in $\mathbf{A^m}$↔**C**. Changes in relative energy are typically less than 0.4 kJ mol^{-1}, except for **A**↔**B**, which is 1 kJ mol^{-1} more stable with the larger basis set. For the controversial **C**→**A** reaction, the basis set enlargement increases the barrier to 10.7 cm^{-1}, whereas the corresponding normal mode of **C** is reduced to 18.5 cm^{-1}.

TABLE II. Torsion angles (degree), relative energies (kJ mol^{-1}), and imaginary frequencies (cm^{-1}) for all local minima and saddle points of the 2-Me-IAA 6-311++G** PES with *syn* orientation of the COOH group. Zero relative energy corresponds to an absolute energy of –627.3238702 Hartree. The superscript »m« is used to denote mirror images. T1, T2, and T3 are the torsion angles C2–C3–C8–C9, C3–C8–C9=O, and H–C10–C2–N1, respectively.

	T1	T2	T3	E_{rel}	ν
A	90.529	–97.882	179.722	0.000	
B	104.997	105.070	179.179	0.151	
C	77.846	–29.094	–171.524	2.821	
A↔**B**	99.788	–175.902	–177.680	7.487	41.78*i*
B↔**C**	104.184	43.877	–179.093	6.471	41.07*i*
A↔**C**	86.761	–44.248	–172.999	2.949	22.06*i*
A↔$\mathbf{B^m}$	172.958	–89.591	178.397	23.655	68.11*i*
$\mathbf{A^m}$↔**C**	4.527	84.169	–14.497	17.024	37.83*i*

DISCUSSION

Several points are noteworthy in the PES of 2-Me-IAA. The first is the extremely low barrier of energy minimum **C** in the reaction to **A**, which has already been mentioned. The barrier height is 0.07 kJ mol^{-1} with 6-31G* and 0.13 kJ mol^{-1} with 6-311++G**. Even if the harmonic approximation is considered too crude a model for a combination of a minimum next to a low-lying transition state, it is clear that vibrational excitation of **C** exceeds the barrier in both cases. **C** therefore cannot be regarded as a stable conformer. The current study has been performed without inclusion of electron correlation, since all previous work in this series has been performed in this manner too. However, inclusion of electron correlation is known to decrease barriers, which is one more argument to classify **C** as unstable. The two stable symmetry unique energy minima **A** and **B** exhibit an energy difference around 0.15 kJ mol^{-1}, almost independent of the basis set employed.

The second noteworthy feature of the 2-Me-IAA PES is the orientation of the methyl group. It is described by a torsion angle T3 close to 180° in most parts of the PES, except for the region around T1 = 0°, where T3 close to 0° is more stable. The mirror symmetrical configurations with T1 = T2 = 0° and T3 = 0° and 180°, which are shown in Figures 6 and 7, are characteristic for this change in methyl group orientation. In the T3 = 180° case, a seven-membered ring H–C–C–C–C–C=O is formed that is closed by a hydrogen bond C=O···H. This ring is of considerable strain, which makes the hydrogen bond weak according to all indicators (*e.g.*, the H-bond distance is 2.120 Å, the 6-31G* bond order[33] is 0.025). In contrast, the T3 = 0° orientation leads to an arrangement with two out-of-plane C=O···H interactions (O···H distances 2.555 Å). As a consequence, the T3 = 0° form is lower in energy than the T3 = 180° form. However, the gain in sterical energy is partially cancelled by the unfavourable, co-planar H–N–C–C–H orientation with parallel bonds N–H and C–H. The net effect is a energy difference between the two forms of 1.9 kJ mol^{-1}.

It should be pointed out that the internal rotation of the methyl group this does not exhibit what sometimes is called »quantum character«, namely several (in this case two) equivalent orientations that are occupied randomly. Instead, if T1 is changed and T2 is kept at a constant value, the methyl group will adopt the energetically most favourable orientation for each combination of T1 and T2. This is done in a smooth internal rotation without sudden changes or jumps.

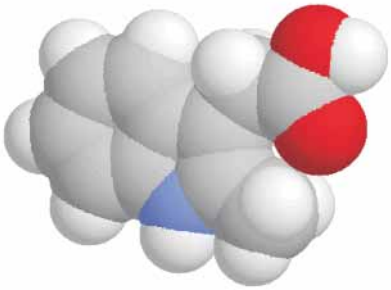

Figure 6. Fused sphere model of the T1 = T2 = T3 = 0° orientation. (T1, T2, and T3 are the torsion angles C2–C3–C8–C9, C3–C8–C9=O, and H–C10–C2–N1, respectively).

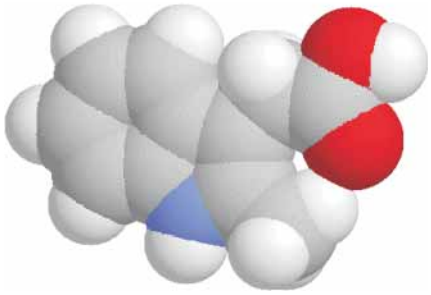

Figure 7. Fused sphere model of the T1 = T2 = 0°, T3 = 180° orientation. (T1, T2, and T3 are the torsion angles C2–C3–C8–C9, C3–C8–C9=O, and H–C10–C2–N1, respectively).

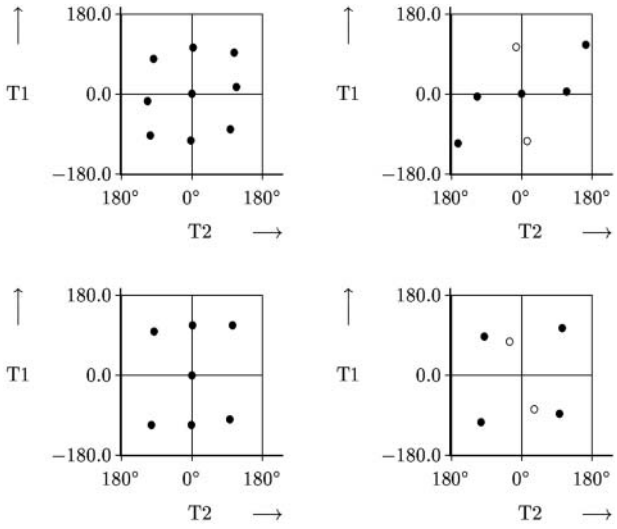

Figure 8. Positions of the local minima in T1/T2-space for 4-Me-IAA (top left), 4-Cl-IAA(top right), IAA (lower left), and 2-Me-IAA (lower right). Stable conformers (•) and vibrationally instable local minima (o) are indicated. (T1 and T2 are the torsion angles C2–C3–C8–C9 and C3–C8–C9=O, respectively).

Comparison with the results for IAA and other derivatives of this compound shows that the methyl group at C2 drastically changes the PES. For IAA and most of its derivatives, the pattern of conformers in T1/T2-space basically forms a grid with three minima per full rotation of T1 or T2. Some of the grid points can be missing, as Figure 8 shows for IAA, 4-Me-IAA, and 4-Cl-IAA. The pattern for 2-Me-IAA, however, basically forms a grid with only two minima per full rotation of T1 or T2. As a consequence, the T1 = T2 = 0° structure, which is a local minimum (in fact, the global minimum in most cases) for IAA or derivatives with either alkyl or halogen sub-

stituents at positions 4, 5, and 6, is a second order saddle point (*i.e.*, a maximum in T1/T2-space) in the case of 2-Me-IAA. Apparently, the conformational entropy of IAA and its alkyl and halogen derivatives substituted at positions 4, 5, 6, and 7 is significantly larger than that of 2-Me-IAA.

Despite the predominant pattern of two minima per full rotation of T1 or T2, a fit of the PES grid point data to trigonometric functions up to fourth order is insufficient: it does yield three symmetry unique local minima in T1/T2 space, but at positions that differ significantly from the RHF optimized geometries. Fits up to sixth or ninth order yield two symmetry unique local minima, which correspond to **A** and **B**. **C** is no local minimum with these PES representations, which therefore give a well-filtered picture.

Specifically, a least squares fit to trigonometric functions up to sixth order results in the following representation (correlation 0.9988):

E_{rel} (kJ mol^{-1}) = + 14.2034 – 0.9992cos(T1) + 11.2820 cos(2T1) – 2.1156cos(3T1) + 1.2369cos(4T1) – 0.1359 cos(6T1) – 2.8086cos(T2) + 2.7187cos(2T2) – 1.6681cos (3T2) – 0.1763cos(4T2) + 0.0875cos(6T2) – 0.7572cos (T1)cos(T2) + 0.7438sin(T1)sin(T2) + 1.8991cos(2T1) cos(2T2) + 0.0003sin(2T1)cos(2T2) – 3.9719sin(2T1)sin (2T2) + 0.0666cos(3T1)cos(3T2) – 0.0430sin(3T1) sin(3T2) + 0.4912cos(4T1)cos(4T2) – 0.4884sin(4T1) sin(4T2) + 0.0875cos(6T1)cos(6T2) – 0.0797sin(6T1) sin(6T2) – 0.5000cos(T1)cos(2T2) + 0.7820sin(T1)sin(2T2) – 0.0219cos(T1)cos(3T2) + 0.0494sin(T1)sin(3T2) + 0.0397 cos(T1)cos(4T2) + 0.0644sin(T1)sin(4T2) – 2.1234cos(2T1) cos(T2) + 3.5234sin(2T1)sin(T2) + 0.4594cos(3T1) cos(T2) – 0.5512sin(3T1)sin(T2) + 0.2461cos(4T1)cos(T2) + 0.3812sin(4T1)sin(T2) – 0.5875cos(2T1)cos(3T2) + 0.5820sin(2T1)sin(3T2) + 0.4922cos(2T1)cos(4T2) + 0.0003sin(2T1)cos(4T2) + 0.0695sin(2T1)sin(4T2) + 0.4241cos(3T1)cos(2T2) – 0.4039sin(3T1)sin(2T2) + 2.2116cos(4T1)cos(2T2) – 2.8844sin(4T1)sin(2T2) – 0.0069cos(3T1)cos(4T2) – 0.0500sin(3T1)sin(4T2) – 0.6531cos(4T1)cos(3T2) + 0.6227sin(4T1)sin(3T2) – 0.0086cos(T1)cos(6T2) – 0.0219sin(T1)sin(6T2) + 0.0594 cos(6T1)cos(T2) + 0.0008sin(6T1)cos(T2) – 0.0656sin(6T1) sin(T2) + 0.0022cos(2T1)cos(6T2) + 0.0003sin(2T1) cos(6T2) – 0.0888sin(2T1)sin(6T2) + 0.3937cos(6T1) cos(2T2) – 0.2903sin(6T1)sin(2T2) – 0.0227cos(3T1)cos (6T2) + 0.0234sin(3T1)sin(6T2) – 0.1638cos(6T1)cos(3T2) + 0.0008sin(6T1)cos(3T2) + 0.1703sin(6T1)sin(3T2) + 0.1016cos(4T1)cos(6T2) – 0.0819sin(4T1)sin(6T2) + 0.2297cos(6T1)cos(4T2) – 0.2398sin(6T1) sin(4T2).

The influence of the methyl group at C2 also extends to the reaction path network. A significant feature in this network are paths with coupled torsions T1 and T2. Such paths are present in the PES of all IAA derivatives. However, for IAA or derivatives with substituents at positions 4, 5, and 6, the torsion coupling is caused by hydrogen bonds, whereas in the case of 2-Me-IAA it is caused primarily by a steric hindering between the methyl and the carboxyl group. Consequently, the energy of the equivalent transitions is higher for 2-Me-IAA than the other indole auxins considered.

Recently Woo *et al.*[28] determined the crystal structure of ABP1 alone and its complex with 1-naphtalene acetic acid (1-NAA). In the crystal structure of the ABP1-1-NAA complex, 1-NAA is bound in the hydrophobic pocket and bidentately coordinates the zinc ion. Inclination of its carboxyl side chain to the conjugated ring plane is about 30°. However, according to the docking study performed,[34] indole auxins can easily bind into the ABP1 active site in a few different orientations and conformations with the carboxyl side chain inclination to the conjugated ring plane ranging from about 10° to 100°. Since 2-Me-IAA cannot easily adopt all these conformations, its binding into the active site of ABP1 is less efficient than the binding of the other indole auxins discussed. The obtained results correlate well with the binding affinity measurements by Rescher *et al*.[29]

Solvation can significantly influence PES[35] of systems involving carboxyl groups. To determine PES of 2-Me-IAA in water, either discret water molecules around the carboxyl group or SCRF should be utilised.

Acknowledgement. – We gratefully acknowledge financial support from the Austrian-Croatian cooperation (Ministry of Science and Technology of the Republic of Croatia and ÖAD-Projekt Nr 15/2002).

REFERENCES

1. P. J. Davies, *Plant Hormones and their Role in Plant Growth and Development*, Martinus Njihoff, Dordrecht, 1987.
2. K. V. Thimann, *Hormone Action in the Whole Life of Plants*, Univ. of Massachusetts Press, Amherst, MA, 1977.
3. S. Marumo, H. Abe, H. Hattori, and K. Munakata, *Agric. Biol. Chem*. **32** (1986) 117–118.
4. S. Marumo, H. Hattori, H. Abe, and K. Munakata, *Nature* (London) **219** (1968) 959–960.
5. S. Marumo, H. Hattori, and H. Abe, *Analyt. Biochem*. **40** (1971) 488–490.
6. K. C. Engvild, H. Egsgaard, and E. Larsen, *Physiol. Plant*. **42** (1978) 365–368.
7. M. Hofinger and M. Böttger, *Phytochemistry* **18** (1979) 653–654.
8. K. C. Engvild, *Physiol. Plant*. **48** (1980) 435–438.
9. E. Ernsten and G. Sandberg, *Physiol. Plant*. **68** (1986) 511–518.
10. R. M. Muir and C. Hansch, *Plant. Physiol*. **28** (1953) 218–232.
11. O. L. Hoffmann, S. W. Fox, and M. W. Bullock, *J. Biol. Chem*. **196** (1952) 437–441.
12. W. L. Porter and K. V. Thimann, *Phytochemistry* **4** (1965) 229–234.
13. M. Böttger, K. C. Engvild, and H. Soll, *Planta* **140** (1987) 89–92.

14. G. F. Katekar and A. E. Geissler, *Phytochemistry* **21** (1982) 257–260.
15. G. F. Katekar and A. E. Geissler, *Phytochemistry* **22** (1983) 27–31.
16. G. Stenlid and K. C. Engvild, *Physiol. Plant*. **70** (1987) 109–113.
17. T. Hatano, M. Katayama, and S. Marumo, *Experientia* **43** (1987) 1237–1239.
18. D. M. Reinecke, J. A. Ozga, and V. Magnus, *Phytochemistry* **40** (1995) 1361–1366.
19. M. Katayama, Y. Kato, H. Kimoto, and S. Fuji, *Experientia* **51** (1995) 721–724.
20. G. K. Munday and A. DeLong, *Trends Plant Sci.* **6** (2001) 534–541.
21. M. Ramek, S. Tomić, and B. Kojić-Prodić, *Int. J. Quant. Chem.: Quant. Biol. Symp*. **22** (1995) 75–81.
22. M. Ramek, S. Tomić, and B. Kojić-Prodić, *Int. J. Quant. Chem.* **60** (1996) 1727–1733.
23. M. Ramek and S. Tomić, *J. Mol. Struct. (Theochem)* **454** (1998) 167–173.
24. M. Ramek and S. Tomić, *Int. J. Quant. Chem*. **70** (1998) 1169–1175.
25. S. Tomić, M. Ramek, and B. Kojić-Prodić, *Croat. Chem. Acta* **71** (1998) 511–525.
26. M. Ramek and S. Tomić, *Int. J. Quant. Chem*. **75** (1999) 1003–1008.
27. M. Ramek and S. Tomić, *Spectrochim. Acta* **A 57** (2001) 1951–1957.
28. E.-J. Woo, J. Marshall, J. Bauly, J.-G. Chen, M. Venis, R. M. Napier, and W. Pickersgill, *The EMBO J*. **21** (2002) 2877–2885.
29. U. Rescher, A. Walther, C. Schiebl, and D. Klämbt, *J. Plant Growth Regul*. **15** (1996) 1–3.
30. S. Antolić, E. Dolušić, E. Kožić, B. Kojić-Prodić, V. Magnus, M. Ramek, and S. Tomić, *J. Plant Growth Regul*. **39** (2003) 235–252.
31. M. W. Schmidt, K. K. Baldridge, J. A. Boatz, S. T. Elbert, M. S. Gordon, J. H. Jensen, S. Koseki, N. Matsunaga, K. A. Nguyen, S. Su, T. L. Windus, M. Dupuis, and J. A. Montgomery, Jr., *J. Comp. Chem*. **14** (1993) 1347–1363.
32. C. C. J. Roothaan, *Rev. Mod. Phys*. **23** (1951) 69–89.
33. I. Mayer, *Chem. Phys. Lett*. **97** (1983) 270–274.
34. B. Bertoša, B. Kojić-Prodić, R. C. Wade, M. Ramek, S. Piperaki, A. Tsantili-Kakoulidou, and S. Tomić, *J. Chem. Inf. Comput. Sci*. **43** (2003) 1532–1541.
35. J. Mavri and D. Hadži, *J. Mol. Struct. (Theochem)* **432** (1998) 257–262.

SAŽETAK

Studiranje 2-metilindol-3-octene kiseline pomoću *ab initio* Hartree-Fockove metode

Michael Ramek i Sanja Tomić

Studirana je ploha potencijalne energije 2-metilindol-3-octene kiseline pomoću *ab initio* Hartree-Fockove metode s dva bazna skupa RHF/6-31G* i RHF/6-31G++G**. S ova dva skupa dobivena su samo 3 simetrijski jednoznačno određena lokalna minimuma na plohi potencijalne energije sa *syn* orijentacijom COOH skupine. Mreža reakcijskih staza povezuje te energijske minimume. Jedan simetrijski jednoznačan energijski minimum ima iznimno malu barijeru do susjednoga globalnoga minimuma. Usporedba s indol octenom kiselinom i njezinim alkiliranim i halogeniranim derivatima sa supstituentima na položajima 4, 5, 6 i 7 pokazuje da je ploha potencijalne energije 2-metilindol-3-octene kiseline sasvim različita. To je u skladu sa značajno nižom aktivnošću auksina i slabijim vezivanjem na protein koji vezuje auksin.